Electronic Supplementary Information

Hydrophilic conjugated polymers additives in fullerene-heterojunction photocatalytic system for efficient photocatalytic hydrogen evolution

Li Tian*[a], Shukui Guo [a], Lingwei Feng[b], Jichao Wang[c], Airong Wang [c*], Cheng-xing Cui[c]

a. School of Materials Science and Engineering, Henan University of Technology, Zhengzhou 450001, P.R. China

b. Institute of Polymer Optoelectronic Materials and Devices, State Key Laboratory of Luminescent Materials and Devices, South China University of Technology, Guangzhou, 510640, P. R. China

c. School of Chemistry and Chemical Engineering, Institute of Computational Chemistry, Henan Institute of Science and Technology, Xinxiang 453003, P. R. China

1. Experimental section

1.1 Materials and synthesis

All chemicals without special explanation were brought from Tianjin Kermel Chemical Reagent Co., Ltd. $PC_{61}BM$, EH-IDTBR, $Pd_2(dba)_3$ and $P(o\text{-}tol)_3$ were purchased from Sigma-Aldrich LLC. and used with no more treatment. Acetic acid thieno [3,4-b] thiophen-2-yl ester was brought from SunaTech Inc. Benzo[1,2-b:4,5-b']dithiophene-4,8-dione, 2-ethylhexano and tetraethyleneglycol monomethyl ether were brought from Energy Chemical. M5[1] was synthesized referencing the

published literatures. The synthetic steps of P4EOBDT-TTE and monomers are presented in **Scheme S1.**

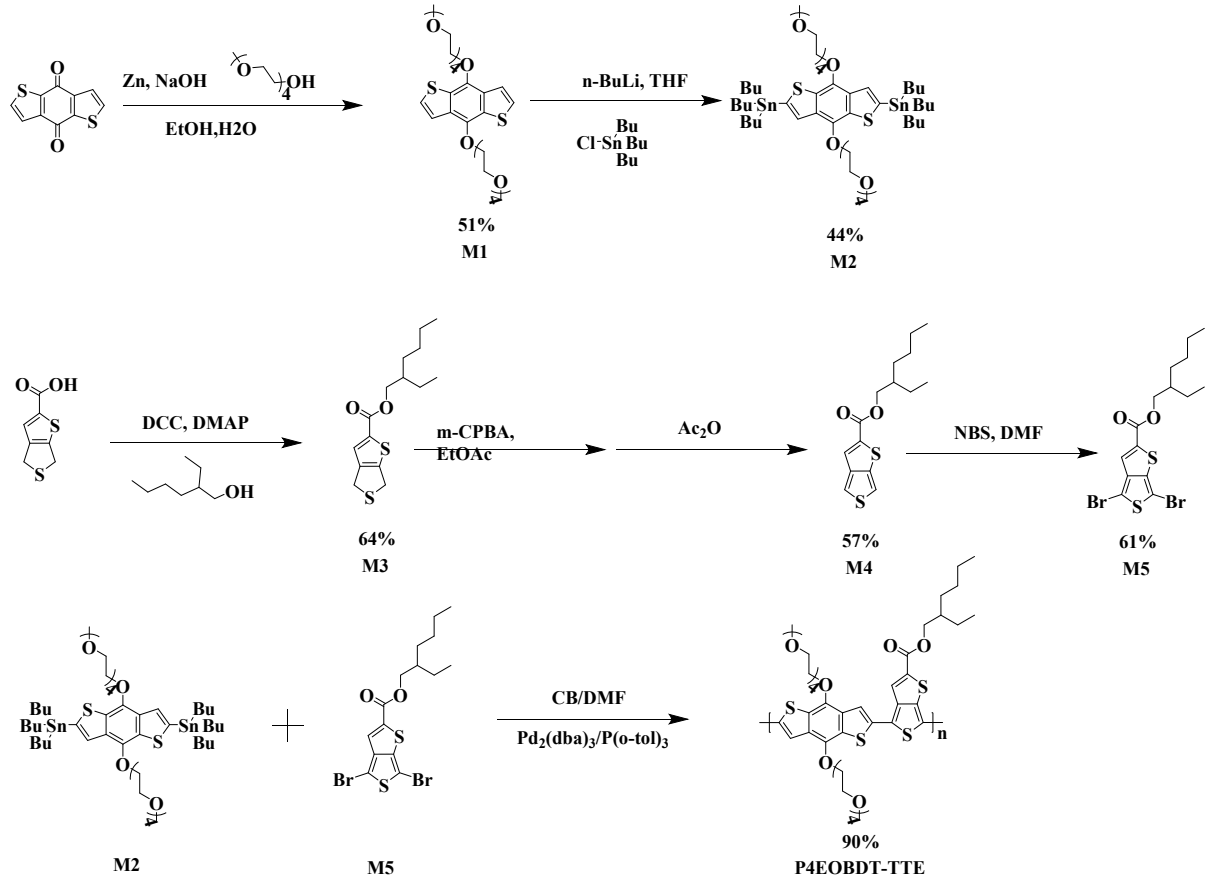

Scheme S1 Synthetic routes of P4EOBDT-TTE.

4,8-bis((2,5,8,11-tetraoxatridecan-13-yl)oxy)benzo[1,2-b:4,5-b']dithiophene (M1)

In a 500 mL two neck flask, benzo[1,2-b:4,5-b']dithiophen-4,8-dione 9 (22.03 g, 100 mmol), of zinc (14.30 g, 220 mmol) were suspended in 150 mL of a solvent mixture of EtOH and H_2O (5:1). NaOH (20 M aqueous solution, 50 mL) was slowly added to the reaction mixture. The reaction mixture was refluxed for 2 h. After cooling to room temperature, 60 mL, etraethyleneglycol monomethyl ether (300.00 mmol) and 0.20 g of the phase transfer catalyst NBu4Br was added. The mixture was heated to reflux for 16 h. After the reaction was finished, 50 mL of water was added to the reaction mixture. The orange mixture was extracted with ethyl acetatee and water, washed by water for two times. The organic phase was then dried with anhydrous $MgSO_4$, and

was evaporated under vacuum to obtain the crude product. After purifying by column chromatography with toluene:ethyl acetate (4:1) as eluent. M1 was obtained as a light brown oil. yield (51 %, 30.74g)

^{1}H-NMR (500MHz, $CDCl_3$, δ ppm):7.62-7.58(d, 2H),7.38-7.37(dd,2H), 4.44-4.42 (m, 4H), 3.88-3.86 (m, 4H), 3.77-3.75 (m, 4H), 3.72-3.69 (m, 4H), 3.68-3.62 (m, 4H), 3.37 (s,6H);

^{13}C-NMR (126 MHz, $CDCl_3$, δ ppm): 142.62, 140.27, 134.28, 132.94, 128.12, 72.48, 71.93, 70.84, 70.73, 70.68, 70.61, 70.55, 70.52, 59.02, 28.99, 27.26, 13.70, 10.86.

4,8-bis((2,5,8,11-tetraoxatridecan-13-yl)oxy)benzo[1,2-b:4,5-b']dithiophenebis (tributylstannane) (M2)

M1 (1.20 g, 2.0mmol) was dissolved in 20 mL of dry THF under -78°C, in an anhydrous flask with nitrogen. Then, n-BuLi (2 mL, 2.5 M in hexane) was dropwise added. The solution was stirred for 1.5 h at -78°C, then tributylchlorostannane (6 mL, 1.0 M in THF) was added slowly. The mixture was stirred at -78 °C for further 30 min and was slowly warmed to room temperature overnight. After quenching with excess of H_2O, the mixture was extracted with dichloromethane. And the organic fraction was washed by water for two times, dried with anhydrous MgSO4, and evaporated under vacuum to obtain the crude product. The crude M2 was further purified by a silica gel column chromatography (the silica gel was soaked in trimethylamine and dried before use) with hexane:methanol (15:1) as eluent. The product was sent to vacuum drying at 60 °C for 24 hours to give a light yellow oil. yield (1.13g，48%).

^{1}H-NMR (500MHz, $CDCl_3$, δ ppm): 7.53 (s, 2H), 4.49-4.41(t, 4H), 3.93-3.88 (t, 4H), 3.77 (m, 4H), 3.71-3.61 (m, 16 H), 3.53- 3.50 (m, 4H), 3.34 (s, 6H), 1.68-1.56 (m, 12H), 1.41-1.33 (m, 12H), 1.24-1.13 (m, 12H), 0.90 (t, 18H).

^{13}C NMR (126 MHz, $CDCl_3$, δ ppm): 142.68, 140.25, 134.28, 132.94, 128.12, 72.48, 71.93, 70.84, 70.75, 70.66, 70.61, 70.53, 70.38, 59.02, 28.87, 27.26, 13.70, 10.86.

2-ethylhexyl 4,6-dibromothieno[3,4-b]thiophene-2-carboxylate (M5)

M5[1] was synthesized according to the reported procedure in reference.

^{1}H-NMR (500MHz, $CDCl_3$, δ ppm): 7.53 (s, 1H), 4.27-4.21(m, 2H), 1.75-1.66 (m, 1H), 1.46-1.32(m, 8H), 0.96-0.90 (m, 6H).

^{13}C NMR (CDCl3, 126MHz), δ (ppm): 199.52, 152.49, 146.22, 140.45, 121.19, 121.15, 103.28, 97.42, 49.43, 32.15, 29.80, 25.92, 22.88, 13.92, 12.02.

Synthesis of P4EOBDT-TTE

In a 15 ml Schlenk reaction tube, M2 (590.0 mg, 0.5 mmol) and M5 (227.0 mg, 0.5 mmol) were dissolved in 5 mL of a solvent mixture of chlorobenzene and DMF (1:1). The mixture was then degassed for three times to remove the oxygen. Then $Pd_2(dba)3$ (1.0 mg) and $P(o\text{-}tol)_3$ (2.0 mg) were added, and the reaction solution was degassed once again. The reaction mixture was stirred under 140℃ in nitrogen atmosphere overnight. After cooling to room temperature, the mixture was then dropped into 200 mL of acetone and the precipitate was collected. After drying, the crude product was extracted using soxhlet extraction from acetone, hexane, and chloroform. The chloroform fraction was then concentrated and precipitated into acetone again. The deep blue solid was collected and dried at 60 ℃ in a vacuum oven for 12 hours.

1H NMR (500 MHz, CDCl3) δ = 7.83 (m, 3H), 4.78 – 4.17 (m, 6H), 4.14 – 3.94 (m, 4H), 3.94 – 3.74 (m, 8H), 3.77 – 3.53 (m, 12H), 3.56 – 3.38 (m, 4H), 3.39 – 3.18 (m, 6H), 1.95 (s, 1H), 1.56 (d, J=60.7, 8H), 1.09 (d, J=46.1, 6H).

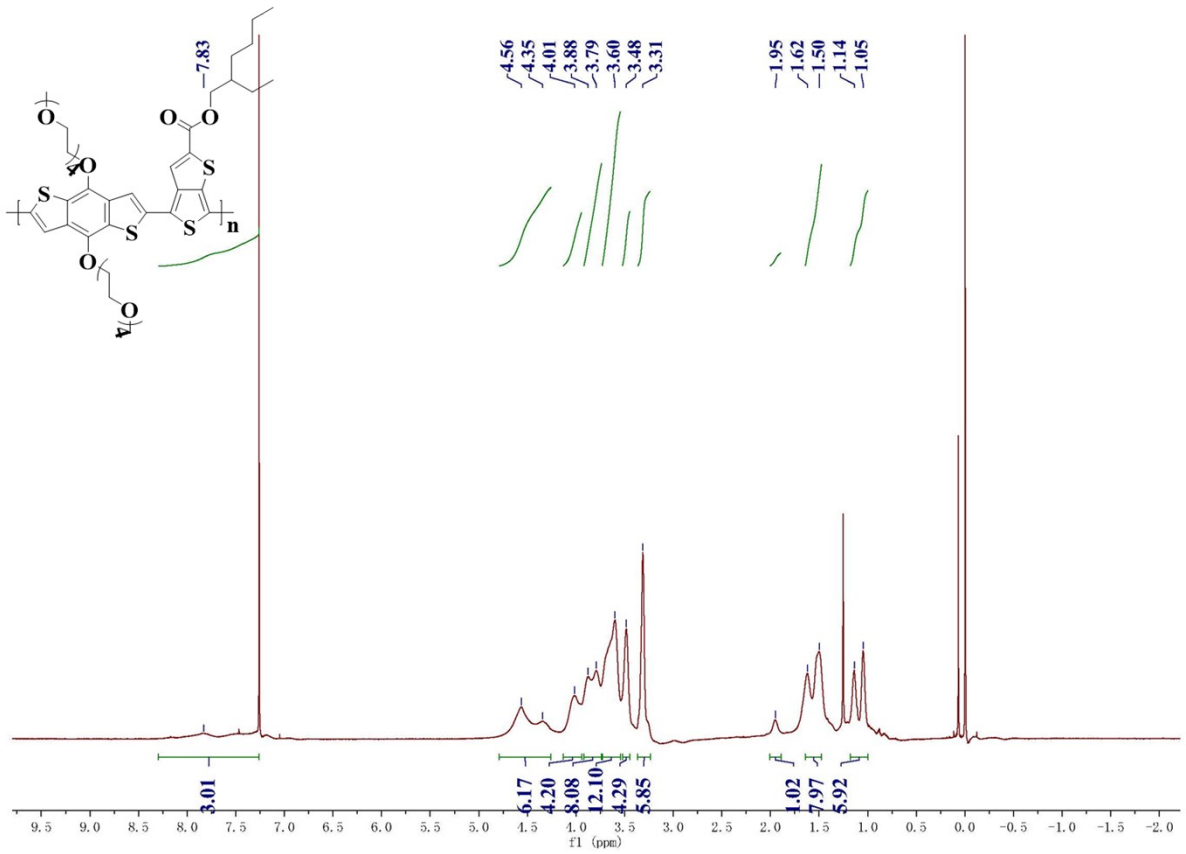

Figure S1 ^{1}H-NMR spectra of P4EOBDT-TTE

1.2 Heterojunction photocatalyst fabrication:

Blend solution for photocatalyst (acceptor: PC61BM or EH-IDTBR) and additive (donor: P4EOBDT-TTE) with the ratio of the desired composition were prepared in 5mL chloroform with a total mass of 1 mg. Then 1.76 g of ascorbic acid was dissolved in 50 mL of deionized water. 5 mL blend solution was quickly injected into ascorbic acid aqueous solution, and then the precursor heterojunction solution was shaken fiercely to form a mini-emulsion. Chloroform solvent was removed by rotary evaporation quickly to obtain a clear solution. After filtration with a 1 μm filter, the heterojunction photocatalyst aqueous solution was diluted to 50 mL with deionized water.

1.3 Equipment and measurement

The ^{1}H NMR spectra and ^{13}C NMR spectra of monomers were measured by Bruker-600 NMR workstation operating at 500 MHz and 126 MHz. The UV-vis absorption spectra of these heterojunction photocatalysts were obtained by using HP 8453 spectrophotometer. The CV curves of heterojunction photocatalysts were recorded by CHI660E electrochemical workstation, in a 0.1

M acetonitrile solution of tetrabutylammonium hexafluorophosphate (Bu_4NPF_6) under the protection of nitrogen at room temperature. A three-electrode setup was used to record the electrochemical characteristics with ITO electrodes modified by heterojunction photocatalysts films as working electrodes, a saturated calomel electrode (SCE) as the reference electrode, and a platinum wire electrode as the counter electrode. The highest occupied molecular orbital (E_{HOMO}) energy levels and the lowest unoccupied molecular orbital (E_{LUMO}) energy levels were calculated as E_{HOMO} =-e(E_{ox}+4.80-E_F) (eV) and E_{LUMO}=-e(-E_{red}+4.80-E_F) (eV), The photoluminescence spectra of these heterojunction photocatalysts, excited at a wavelength of 360 nm and 722 nm, were recorded by an FLS920 spectrofluorimeter. The water contact angle measurements of these heterojunction photocatalysts were performed using a DATAPHYSICS OCA40 Micro surface tension tester. TEM images were obtained from a JEM-2100F instrument.

1.4 Performance test

1.4.1 Hydrogen evolution

Photocatalytic hydrogen production experiments were conducted in a top irradiation reaction vessel with a quartz cell of 50 mL. Hydrogen evolution was measured using 50 mL of prepared heterojunction photocatalyst solution with ascorbic acid as sacrificial electron donor (0.2M, PH=4 adjusted by 1.0 M NaOH solution). 8 wt% Pt co-catalyst was deposited with an in situ photodeposition method. H_2PtCl_4 was added to the sample solution and illuminated for 0.5 h to form Pt nanopaticles as co-catalysts. The reaction unit was sealed with a quartz septum and the resulted reaction mixture was degassed by vacuuming to remove the dissolved oxygen. A Xe lamp (300W, Ceaulight) was used as the light source. The luminous power reaching the surface of the reaction solution was calibrated to be 150 mW cm^{-2} by a power meter. And the hydrogen was recorded by gas chromatography (GC7900II, using Ar as carrier gas). The sensor was standardized by injecting different volumes of hydrogen with the experiment condition. The sensor was polarized at +36 mV until reaching a stable value before every measurement. Finally, the hydrogen evolution rate (HER) of heterojunction photocatalyst for PC61BM/P4EOBDT-TTE and EH-IDTBR/P4EOBDT-TTE with different composition ratios were estimated by linear fitting for H2 evolution vs. time (**Figure S12** and **Figure S13**) .

1.4.2 Apparent quantum yield (AQY) measurement

The AQY measurements were measured in the same condition as hydrogen evolution measurements, but with selected wavelengths using band pass filters (380 nm, 420 nm, 450 nm, 500 nm, 550 nm, 600 nm, 650 nm and700 nm). The sample solution added H_2PtCl_4 was first illuminated under simulated solar light for 0.5 h to complete Pt photodeposition. The light source was fitted with different wavelengths of band pass filter, and the sample solution was illuminated with filtered light within a narrow wavelength range. Each group of test in specific wavelength was repeated 3 times and irradiated for 20 minutes each time. Before each test, the reactor was evacuated and purged with Ar 5 times to remove all the H_2 evolved during last time. The AQY can be calculated from the equation: $EN_0 = \frac{E\lambda T\%}{hc}\lambda T$, $N = \frac{V \times 6.02 \times 1023}{22.4t}$, AQY=$2N/N_0$, N represent the number of incident photons, N_0 represents the number of collected H2 molecules, E represents the energy of incident light at a selected wabelength determined by a calibrated power meter, represents the wavelength of the incident light, V represents the volume of generated H_2 in a certain period of time(t), detected by GC, T% represents the transmittance of the quartz cell.

1.4.3 Photocurrent measurement

The photocurrent measurements were conducted with a CHI660E Electrochemical System in a three-electrode setup with a Pt sheet as the counter electrode and an Ag/AgCl electrode (3 M KCl) as the reference electrode. The working electrodes were prepared by coating heterojunction photocatalyst films (10 mg mL^{-1} in $CHCl_3$) onto ITO glasses with thicknesses about 300 nm. The active area is confined to 0.50 cm^2. A 0.1 M Na_2SO_4 aqueous solution (pH = 6.8) was chosen as the supporting electrolyte and was purged with nitrogen for 30 min to remove O_2 before measurements. A Xe lamp (300W, Ceaulight $\lambda > 300$ nm) was used as the light source. Shutter was used to control illumination interval (bright state for 20 s, dark state for 20 s) repeating 10 circulates.

1.4.4 Photocatalytic stability test

In the photocatalytic stability test, the hydrogen evolution experiment was repeated consecutive 4 runs. The irradiation time of each time is 4 h, before each test, the reactor was evacuated and purged with Ar to remove all the H_2 evolved during last time. After continuous illumination for 20 h, equal amount of sample solution before and after irradiation were evaporated by rotary evaporation. The residues were collected and dried at 70 ℃ in a vacuum oven for 12 hours. Finally,

the residues were characterized through infrared spectroscopy to research the photostability of fullerene-NP.

1.5 Femtosecond transient absorption spectroscopy

Ultrafast TAS analysis of heterojunction photocatalyst dispersed in water was carried out by using a self-built system. Femtosecond laser is generated by an Ti:Sapphire regenerative amplifier (Spitfre Ace, Spectra Physics), with a 800 nm laser pulse (2mJ single pulse energy, 500 Hz repetition rate). The laser pulse is divided into the pump and the probe by using a beam splitter. The pump laser at 355 nm is generated through an optical parametric amplifier (Spectra Physics, TOPAS-Prime). The pump pulse is chopped by a synchronized chopper with a Frequency of 250 Hz. The continuous white light probe in the visible (400−850 nm) region is generated by focusing the probe pulse into a sapphire crystal. Then, the probe pulse is divided before the sample into two pulses, one is directed to the sample and the other is used as the reference. The time delay between the pump laser and the probe pulse is achieved through a computer-controlled motorized translation stage (Newport, ESP300) with a testing time window for 0-2 ns. The variation of transmittance for probe pulse before and after passing through the sample with different delay time is recorded using a CCD-diode array detector (SOL instruments, MS2004i) equipped with a monochromator. The samples were measured in Argon atmosphere. All suspensions were measured at equal numbers of absorbed photons.

1.6 Fabrication of electron-only devices

Electron-only devices were fabricated with device structures of ITO/ZnO/fullerene-HP film (100 nm)/Al. The electron mobility was measured by fitting the dark J-V current to the space charge limited current (SCLC) method. The SCLC method is described as: $J = (9/8)\varepsilon_0\varepsilon_r\mu((V^2)/(d^3))$, where J is the current, μ is the zero-field mobility, ε_0 is the permittivity of free space, ε_r is the relative permittivity of the material, d is the thickness of the fullerene-HP films, and V is the effective voltage. The effective voltage can be obtained by subtracting the built-in voltage (V_{bi}) and the voltage drop (V_s) from the substrate's series resistance from the applied voltage (V_{appl}), $V = V_{appl} - V_{bi} - V_s$. The electron mobility can be calculated by the fitting slope of the $J^{1/2}$-V curve.

2. Analytical Data

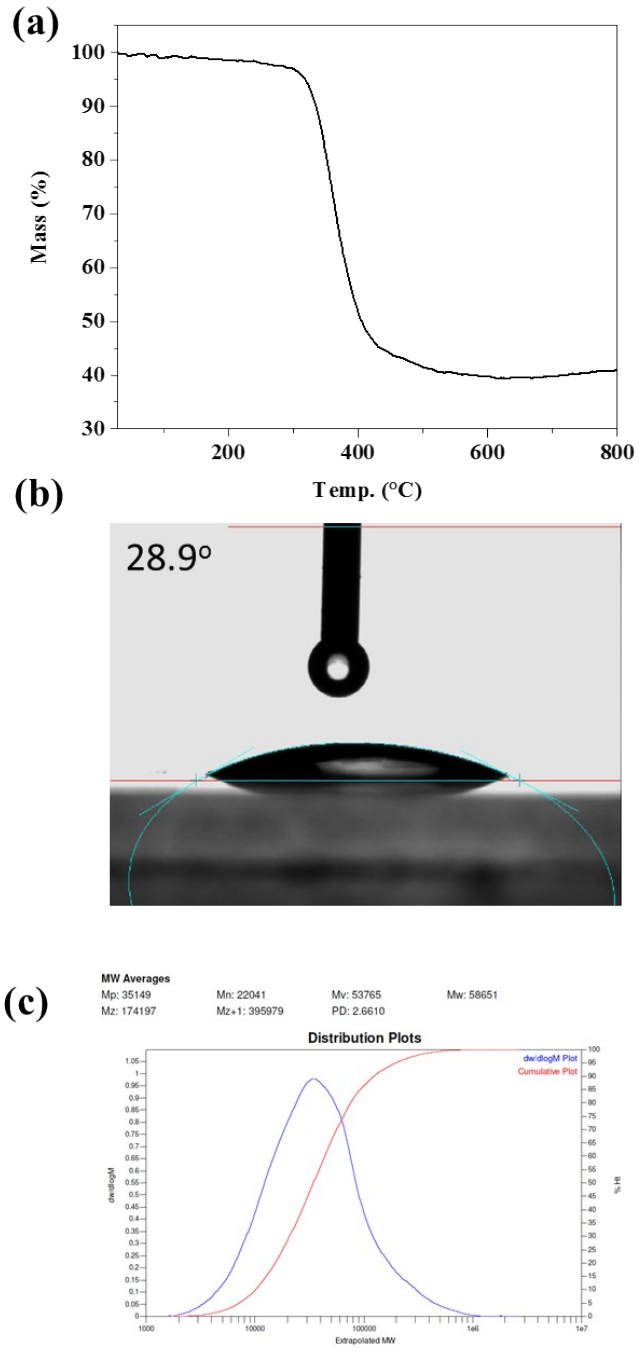

Figure S2 Basic physical properties. a) TGA of P4EOBDT-TTE under nitrogen at a heating rate of 10 °C min^{-1}, b) The water contact angle images of P4EOBDT-TTE, c) GPC of P4EOBDT-TTE with $CHCl_3$ as the eluent using linear polystyrene standards at room temperature.

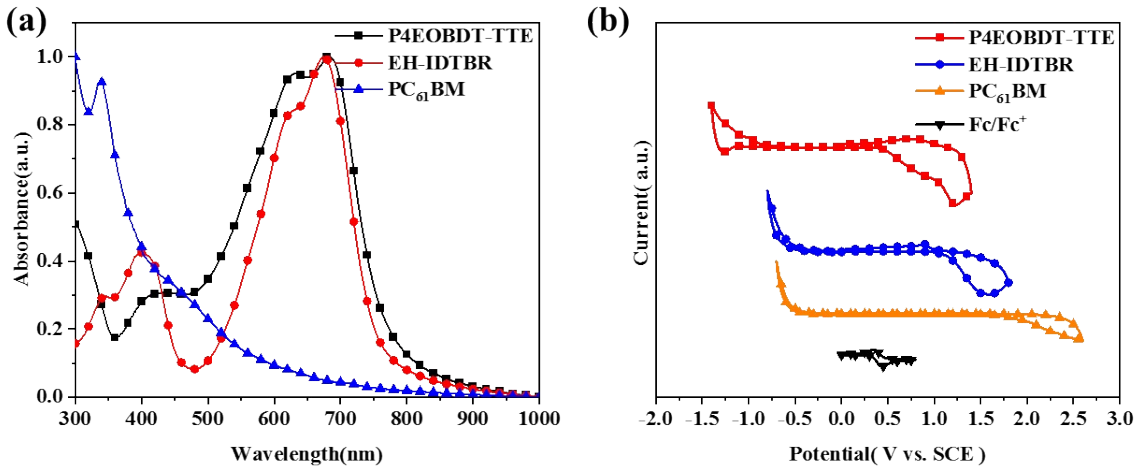

Figure S3 Photoelectric characteristic a) The absorption spectrum images of P4EOBDT-TTE, EH-IDTBR and $PC_{61}BM$ in film state, b) The cyclic voltammetry curves of P4EOBDT-TTE, EH-IDTBR, $PC_{61}BM$ and Fc/Fc+ reference under nitrogen protection.

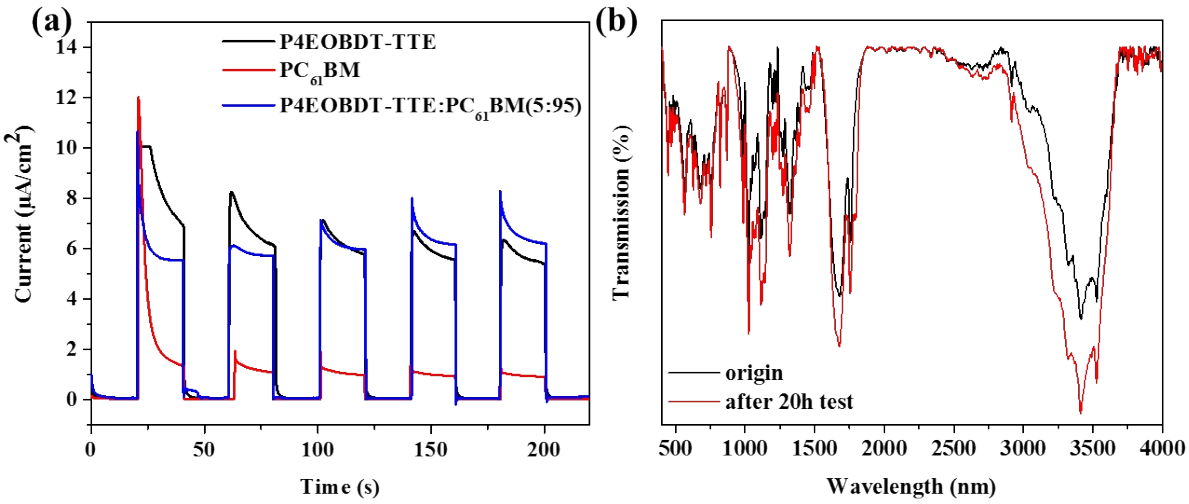

Figure S4 Photocatalytic performance. a) Photocurrent curves of P4EOBDT-TTE, PC61BM and P4EOBDT-TTE:$PC_{61}BM$ 5:95 particles at an applied voltage of 0 V in a standard photoelectron chemical cell with 0.1 M Na_2SO_4 as the electrolyte, b) FT-IR spectrum of P4EOBDT-TTE:PC61BM 5:95 before and after irradiation

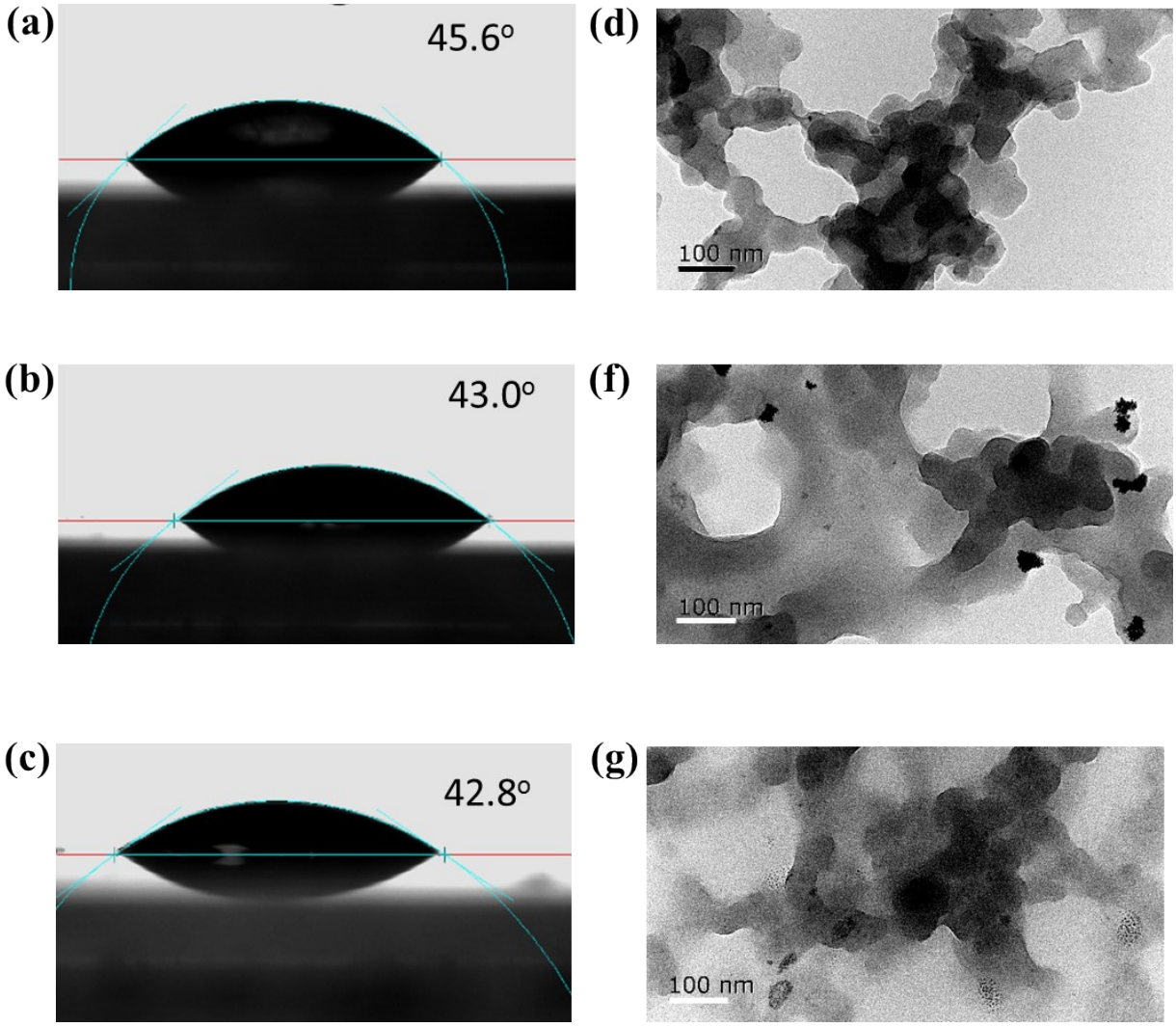

Figure S5. Morphology. The water contact angle images of P4EOBDT-TTE: PC61BM a) 50:50, b) 70:30, c) 95:5. The TEM images of P4EOBDT-TTE: PC61BM e) 50:50, f) 70:30, g) 95:5. The TEM samples were prepared by dropping their diluted aqueous solutions, which were the same as those used for photocatalytic experiments, onto copper grids.

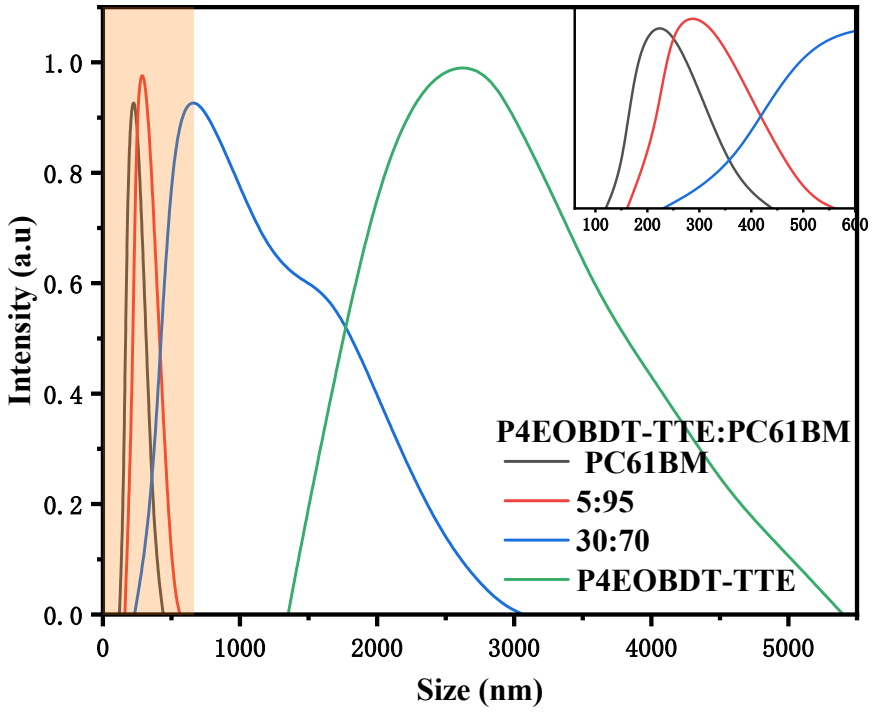

Figure S6:The size distribution of fullerene-HPs

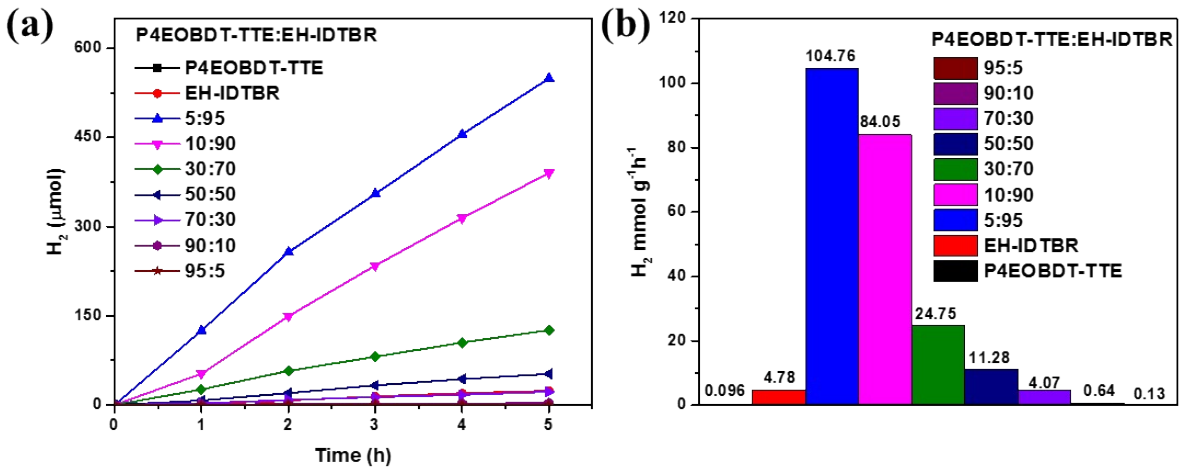

Figure S7. Photocatalytic performance. a) H_2 evolution vs. time for P4EOBDT-TTE:EH-IDTBR particles formed from a range of P4EOBDT-TTE: EH-IDTBR ratios. b) Average H_2 evolution

rates of P4EOBDT-TTE: EH-IDTBR particles over 5 h as a function of the P4EOBDT-TTE to EH-IDTBR blend ratio.

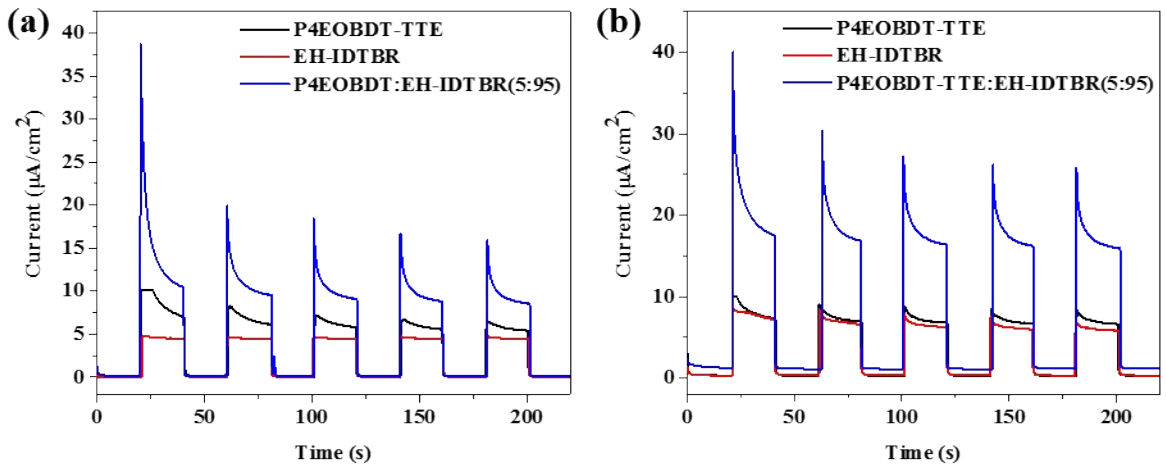

Figure S8. Photocurrent curves. Photocurrent curves of P4EOBDT-TTE, EH-IDTBR and P4EOBDT-TTE: EH-IDTBR 5:95 particles in a standard photoelectron chemical cell with 0.1 M Na_2SO_4 as the electrolyte at an applied voltage of a) 0 V, b) -0.2 V.

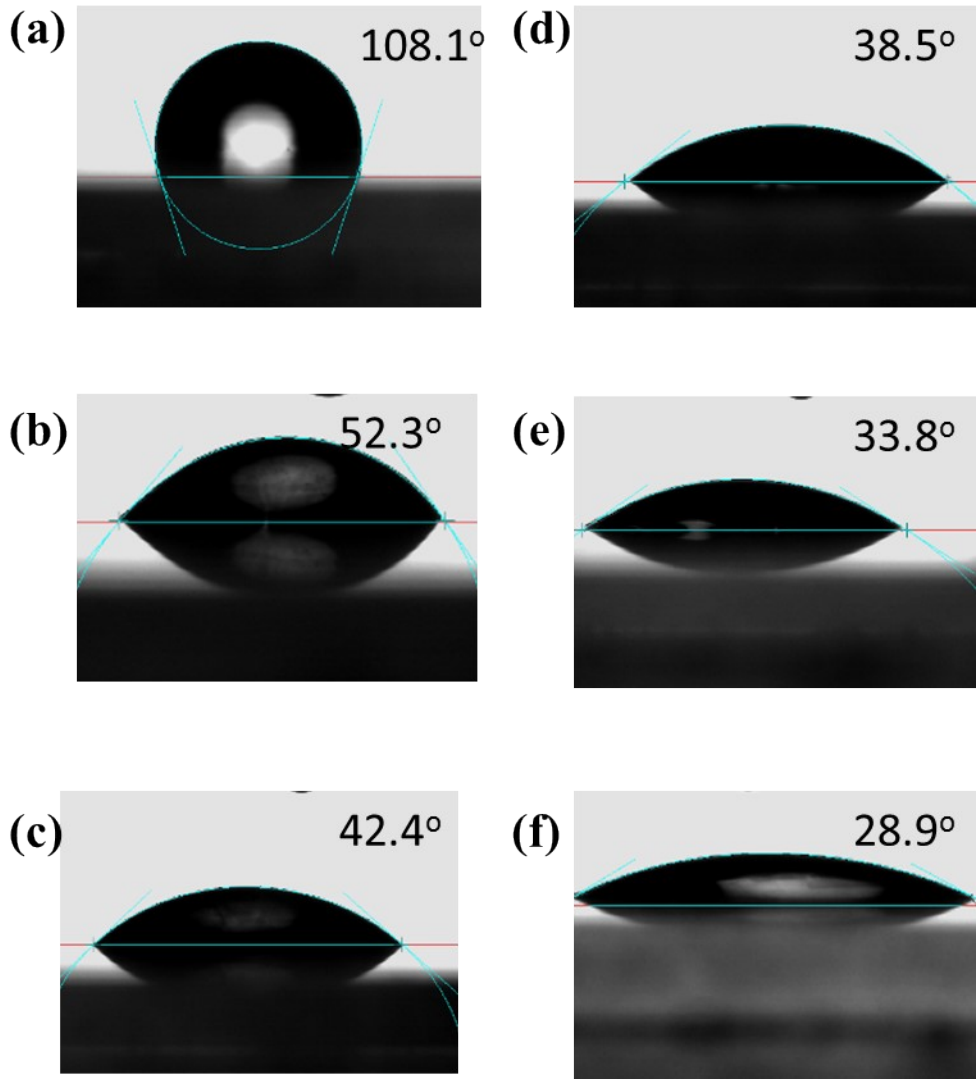

Figure S9. Contact angle. The water contact angle images of a) P4EOBDT-TTE, b) P4EOBDT-TTE: EH-IDTBR 5:95, c) P4EOBDT-TTE: EH-IDTBR 30:70, d) P4EOBDT-TTE: EH-IDTBR 70:30, e) P4EOBDT-TTE: EH-IDTBR 95:5, f) P4EOBDT-TTE.

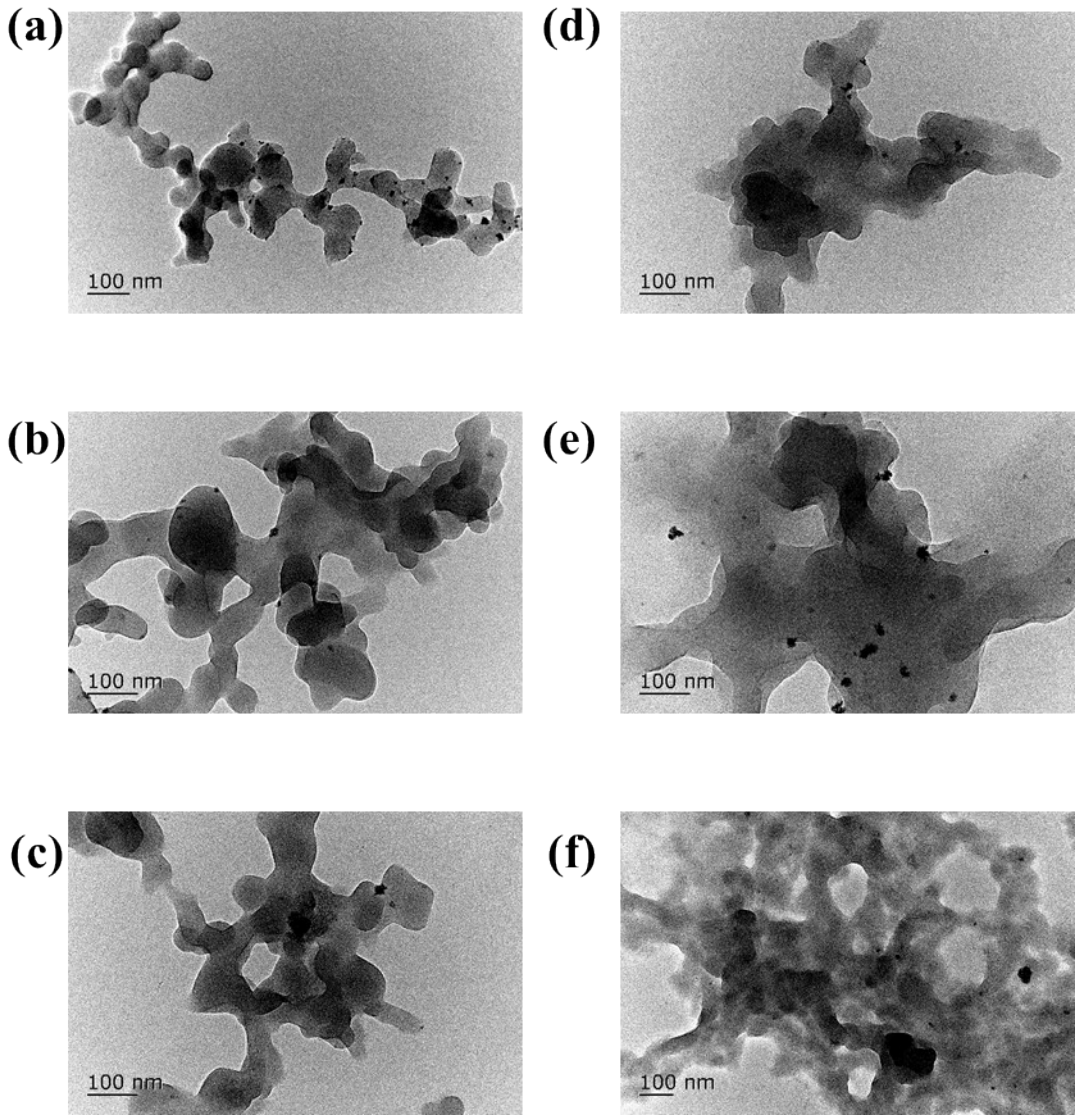

Figure S10. Morphology. The TEM images of a) EH-IDTBR 5:95, b) P4EOBDT-TTE: EH-IDTBR 5:95, c) P4EOBDT-TTE: EH-IDTBR 30:70, d) P4EOBDT-TTE: EH-IDTBR 70:30, e) P4EOBDT-TTE: EH-IDTBR 95:5, f) P4EOBDT-TTE. The TEM samples were prepared by dropping their diluted aqueous solutions, which were the same as those used for photocatalytic experiments, onto copper grids.

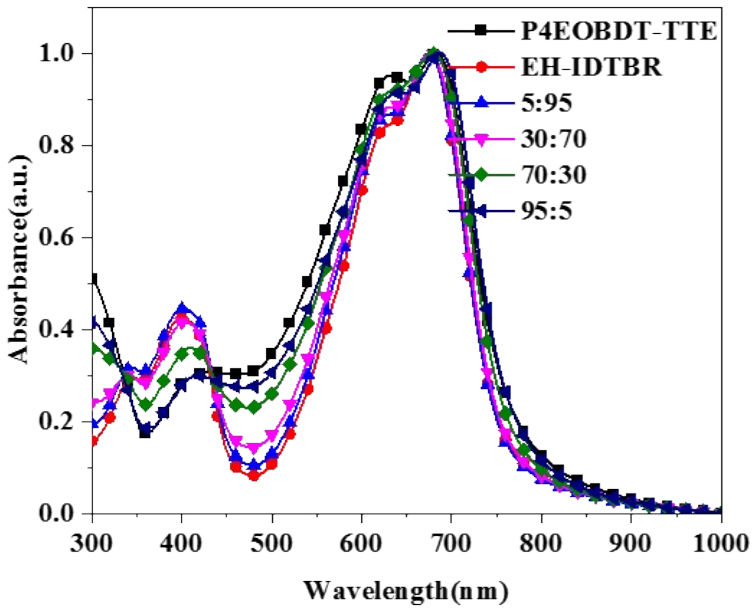

Figure S11. The absorption spectrum images of P4EOBDT-TTE: EH-IDTBR at different composition ratios dispersed in deionized water.

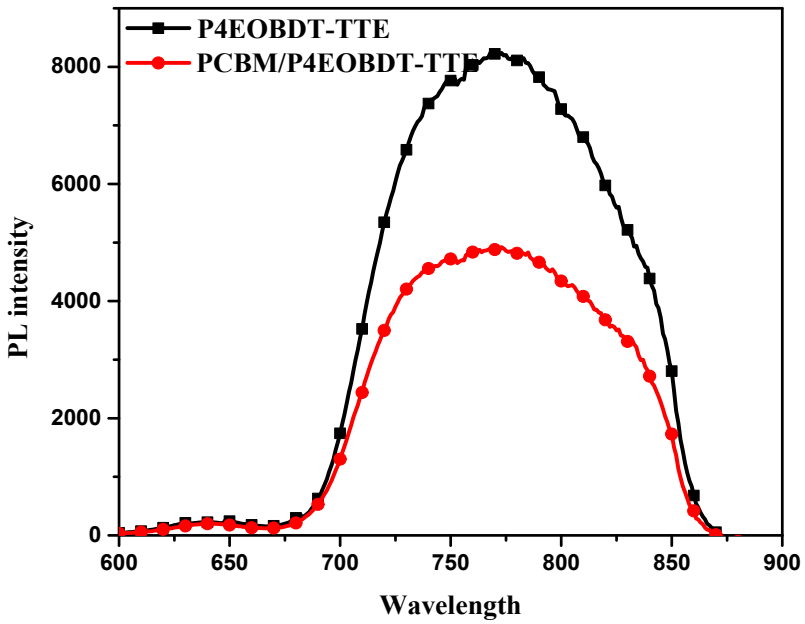

Figure S12. Steady state PL spectra of fullerene-HPs (with 0% and 50% PC61BM) exciting at 540 nm to selectively excite P4EOBDT-TTE.

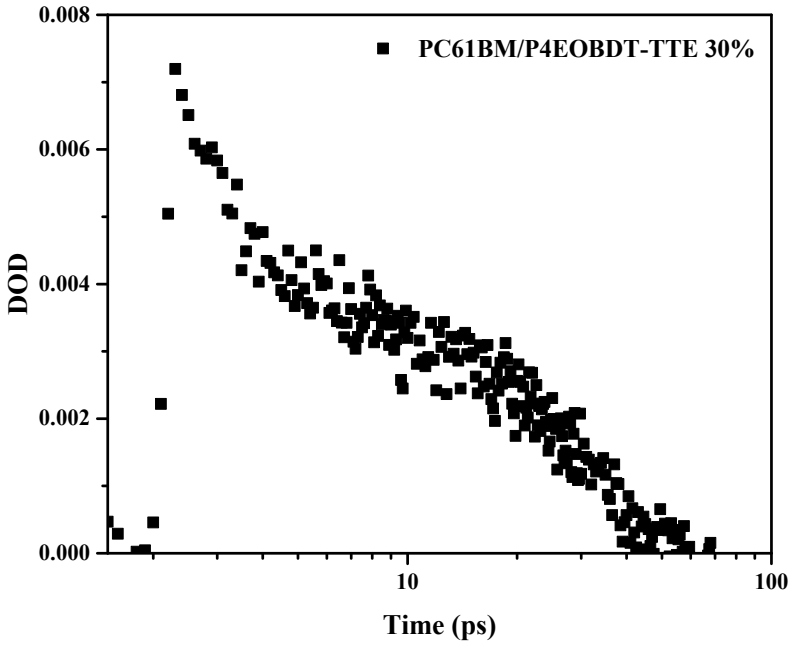

Figure S13. Transient absorption decay dynamics for fullerene-HPs (with 30% P4EOBDT-TTE) excited at 355 nm and probed at 560 nm, assigned to PC61BM exciton decay.

P4EOBDT

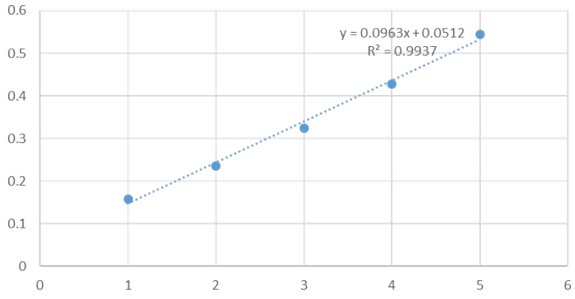

PC61BM

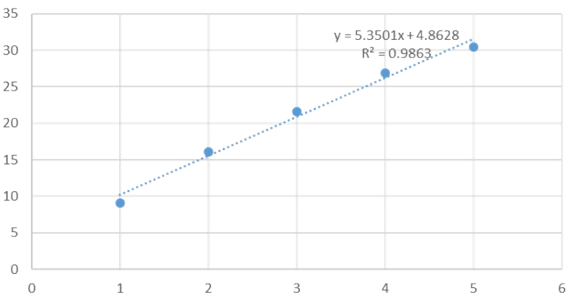

P4EOBDT/PC61BM(5:95)

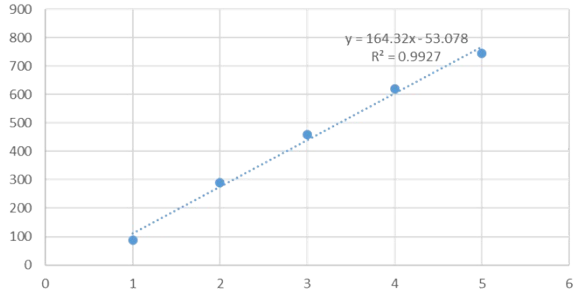

P4EOBDT/PC61BM(10:90)

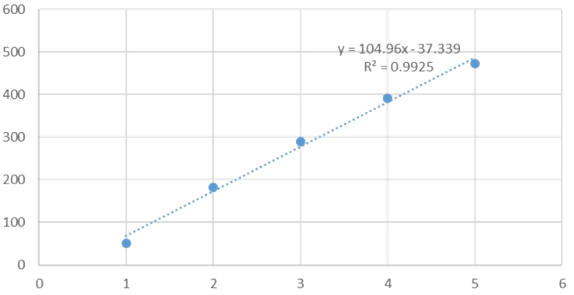

P4EOBDT/PC61BM(30:70)

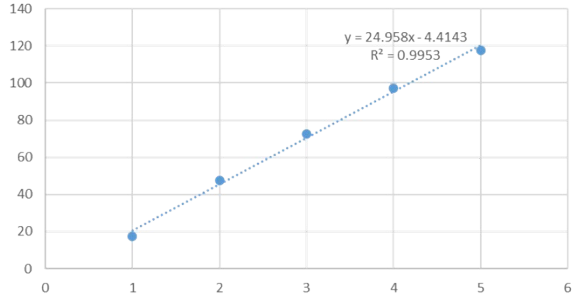

P4EOBDT/PC61BM(50:50)

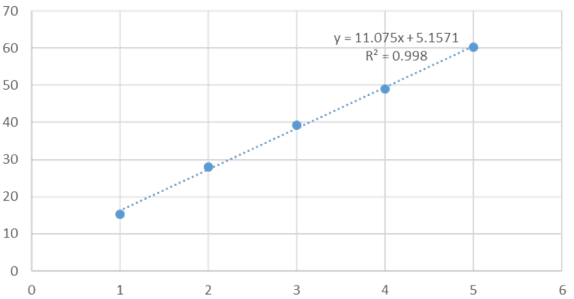

P4EOBDT/PC61BM(70:30)

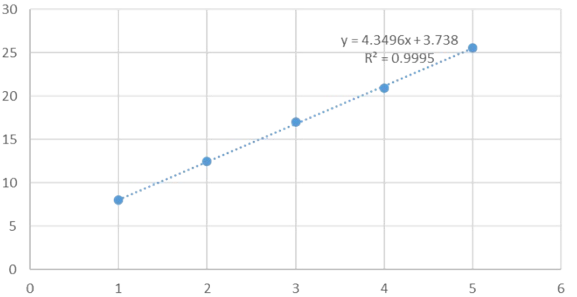

P4EOBDT/PC61BM(90:10)

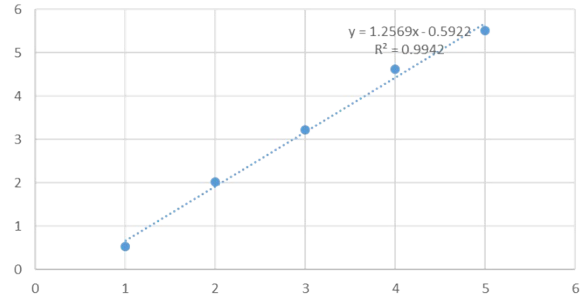

P4EOBDT/PC61BM(95:5)

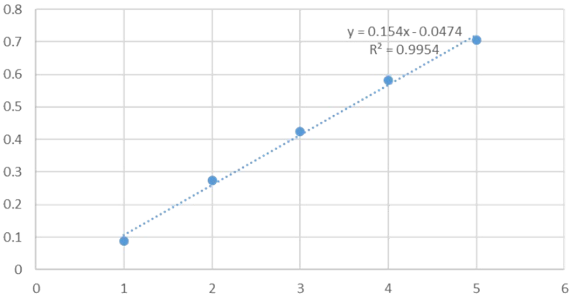

Figure S14. Linear fitting for H_2 evolution vs. time for P4EOBDT-TTE:PC61BM particles formed from a range of P4EOBDT-TTE:PC61BM ratios.

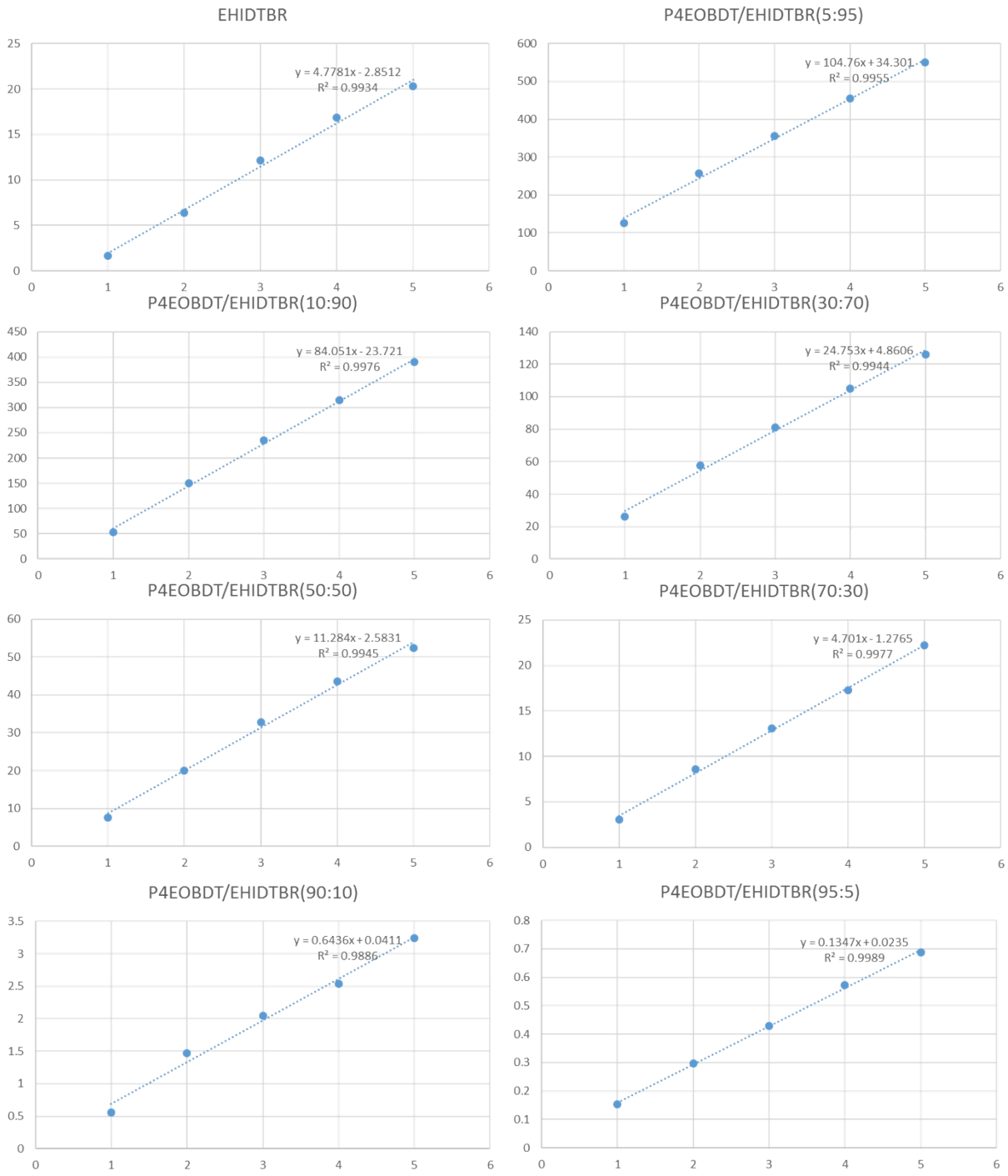

Figure S15. Linear fitting for H_2 evolution vs. time for P4EOBDT-TTE: EH-IDTBR particles formed from a range of P4EOBDT-TTE:PC61BM ratios.

Table S1 Absorption and energy levels of organic semiconductor materials

Molecule	λabs (nm)	Eox (V)	Ere (V)	HOMO(eV)	LUMO (eV)
PC61BM	380	1.7	-0.5	-6.1	-3.9
EH-IDTBR	720	1.2	-0.5	-5.6	-3.9
P4EOBDT-TTE	720	0.5	-0.9	-4.9	-3.5

Table S2 HER of fullerene-HPs (P4EOBDT-TTE: PC61BM)

Molecule	1 h (μ mol)	2 h (μ mol)	3 h (μ mol)	4 h (μ mol)	5 h (μ mol)	HER (mmol/g.h)
PC61BM	9.14	16.20	21.72	26.99	30.50	5.35
P4EOBDT-TTE	0.16	0.24	0.33	0.43	0.55	0.096
5:95	87.40	288.81	460.14	619.31	743.75	164.32
10:90	51.70	182.40	290.07	391.66	471.87	104.96
30:70	17.48	47.59	72.65	97.03	117.55	24.96
50:50	15.36	28.01	39.30	48.99	60.25	11.08
70:30	7.99	12.51	16.98	20.91	25.53	4.35
90:10	0.53	2.01	3.22	4.61	5.51	1.26
95:5	0.09	0.27	0.42	0.58	0.70	0.15

Table S3 The summary of the photocatalytic hydrogen production performances of photocatalysts under AM 1.5G, 100 mW cm^{-2} irradiation.

Catalysts	Co-catalyst	Sacrificial agent	HER (mmol g^{-1} h^{-1})	Rfe.
COF-954	Pt	AA	43.5	2
PM6:Y6	Pt	AA	43.9	3
PM6:TPP	Pt	AA	64.3	4
COF-935	Pt	AA	67.55	5
PM6:PCBM	Pt	AA	73.7	3
DBC-BTDO	Pt	AA	104.86	6
PyBS-3	Pt	AA	105	7
PTA	Pt	AA	118.9	8
Py-T-BTDO-3	Pt	AA	127.9	9
PDBTSO-T	Pt	AA	147	10
ZnSeNR	Pt	AA	149	11
F1	Pt	AA	152.6	12
TP-BTDO-2	Pt	AA	161.28	13
PCBM: P4EOBDT-TTE	Pt	AA	164.32	This work
PM6:Y6CO	Pt	AA	183.5	14
PM6:2FBP-4F	Pt	AA	207.6	15

Table S4 HER of HPs (P4EOBDT-TTE: EH-IDTBR)

Molecule	1 h (μ mol)	2 h (μ mol)	3 h (μ mol)	4 h (μ mol)	5 h (μ mol)	HER (mmol/g.h)
EH-IDTBR	1.67	6.39	12.16	16.87	20.32	4.78
P4EOBDT-TTE	0.16	0.24	0.33	0.43	0.55	0.069
5:95	125.14	257.31	355.12	455.56	549.83	104.76
10:90	52.65	149.62	234.86	314.65	390.39	84.05
30:70	26.03	57.46	81.02	105.11	125.97	24.75
50:50	7.58	20.10	32.86	43.511	52.30	11.28
70:30	3.02	8.57	13.10	17.25	22.19	4.07
90:10	0.56	1.47	2.05	2.54	3.24	0.64
95:5	0.15	0.30	0.43	0.57	0.69	0.13

Reference:

1. Y. Yao, Y. Liang, V. Shrotriya, S. Xiao, L. Yu, Y. Yang, *Adv. Mater.,* 2007, **19**, 3979-3983.
2. Y. Zhong, W. Dong, S. Ren, L. Li, *Adv. Mater.* 2024, **36**, 2308251.
3. J. Kosco, S. Gonzalez-Carrero, C. T. Howells, T. Fei, Y. Dong, R. Sougrat, G. T. Harrison, Y. Firdaus, R. Sheelamanthula, B. Purushothaman, F. Moruzzi, W. Xu, L. Zhao, A. Basu, S. De Wolf, T. D. Anthopoulos, J. R. Durrant, I. McCulloch, *Nat. Energy* 2022, **7**, 340-351.
4. Z. Zhang, W. Si, B. Wu, W. Wang, Y. Li, W. Ma, Y. Lin, *Angew. Chem. Int. Ed.* 2022, **61**, e202114234.
5. K. Wang, Y. Zhong, W. Dong, Y. Xiao, S. Ren, L. Li, *Angew. Chem. Int. Ed.* 2023, **62**, e202304611.

6. C. Han, S. Xiang, M. Ge, P. Xie, C. Zhang, J.-X. Jiang, *Small* 2022, **18**, 2202072.

7. C. Shu, C. Han, X. Yang, C. Zhang, Y. Chen, S. Ren, F. Wang, F. Huang, J.-X. Jiang, *Adv. Mater.* 2021, **33**, 2008498.

8. Y. Guo, Q. Zhou, J. Nan, W. Shi, F. Cui, Y. Zhu, *Nat. Commun.* 2022, **13**, 2067.

9. C. Han, S. Xiang, P. Xie, P. Dong, C. Shu, C. Zhang, J.-X. Jiang, *Adv. Funct. Mater.* 2022, **32**, 2109423.

10. Y. Liu, J. Wu, F. Wang, *Appl. Catal., B* 2022, **307**, 121144.

11. M. F. Kuehnel, C. E. Creissen, C. D. Sahm, D. Wielend, A. Schlosser, K. L. Orchard, E. Reisner, *Angew. Chem. Int. Ed.* 2019, **58**, 5059-5063.

12. Y. Zhu, Z. Zhang, W. Si, Q. Sun, G. Cai, Y. Li, Y. Jia, X. Lu, W. Xu, S. Zhang, Y. Lin, *J. Am. Chem. Soc.* 2022, **144**, 12747-12755.

13. C. Han, S. Xiang, S. Jin, L.-W. Luo, C. Zhang, C. Yan, J.-X. Jiang, *J. Mater. Chem. A* 2022, **10**, 5255-5261.

14. Y. Liang, T. Li, Y. Lee, Z. Zhang, Y. Li, W. Si, Z. Liu, C. Zhang, Y. Qiao, S. Bai, Y. Lin, *Angew. Chem. Int. Ed.* 2023, **62**, e202217989.

15. Z. Zhang, C. Xu, Q. Sun, Y. Zhu, W. Yan, G. Cai, Y. Li, W. Si, X. Lu, W. Xu, Y. Yang, Y. Lin, *Angew. Chem. Int. Ed.* 2024, **63**, e202402343.